Electrochemical assessment of pigment-binding-pigment interactions in oil paint deterioration: a case study on indigo and Prussian blue

Antonio Doménech-Carbó (antonio.domenech@uv.es)
Universitat de Valencia https://orcid.org/0000-0002-5284-2811
María Teresa Doménech-Carbó
Universidad Politecnica de Valencia
Laura Osete-Cortina
Universitat Politècnica de València
Margherita Donnici
Universita Ca' Foscari
Nuria Guasch-Ferré
Universitat de Barcelona Facultat de Medicina i Ciencies de la Salut
Rosa M. Gasol-Fargas
Diputació de Barcelona
Manuel Ángel Iglesias-Campos
Universitat de Barcelona

Research article

Keywords: Electrochemistry, Oil paints, Prussian blue, Indigo, Deterioration

Posted Date: April 28th, 2020

DOI: https://doi.org/10.21203/rs.3.rs-23531/v1

Version of Record: A version of this preprint was published on July 16th, 2020. See the published version at https://doi.org/10.1186/s40494-020-00415-x.

Abstract

The degradation of synthetic oil paint film specimens containing indigo and Prussian blue pigments and pictorial samples from the *Sant Francesc de Paula* painting from the museum of Cardedeu (Catalonia, Spain) has been studied by voltammetry of immobilized particles. This technique, combined with SEM-EDX, ATR-FTIR and CG-MS techniques permits to propose a dual scheme for the degradation of the pigments when submitted to natural, UV and UV solar light aging. Under 'ordinary' conditions, Prussian blue acts as a radical scavenger moderating the production of ROS produced in the binding media by the action of UV radiation, resulting in the formation of Berlin green and indigo adducts with radicals. In the case of localized areas of the *Sant Francesc de Paula* paint, strong degradation occurs where Prussian blue acts as a promoter of the indigo oxidation to isatin, thus resulting in a considerable chromatic shift.

1. Introduction

The deterioration of oil paintings is a complex problem due to the variety of organic and inorganic materials constitutive of pictorials layers and the action of different types of external agents, including the light, humidity, microorganisms and mechanical and thermal stress [1–4]. The deterioration of oil films is associated to crosslinking reactions, oxidation of unsaturated acids and hydrolysis of glyceride bonds releasing free fatty acids. The role of pigments in such deterioration processes has received considerable attention due to their possible role as inhibitors or catalysts of oil drying [2, 5–7], formation of metal soaps [8–12], and mineralization [9, 12].

In order to study oil paints degradation processes, a variety of analytical techniques have been used, including, among others, image analysis [13], infrared spectroscopy [5, 11, 14, 15], scanning electron microscopy image analysis [12], Raman spectroscopy [16].

The interaction between pigments and oils has been subject of different studies, concentrated in lead pigments [12, 13, 17, 18] and Prussian blue [19], the role of the mutual pigment-oil interactions being to some extent controversial [20–22].

In this context, the voltammetry of immobilized particles (VIMP), a solid state electrochemistry technique developed by Scholz et al. [23–25], can be applied due to its sensitivity to different redox states and its ability to work with samples at the level of few nanograms. These characteristics prompt the application of VIMP in the fields of archaeometry, conservation and restoration, as summarized in different reviews [26–28]. In previous works, we have described the use of VIMP to characterize the biodegradation of cadmium yellow [29] and verdigris [30] pigments in reconstructed egg tempera and egg-linseed oil emulsion paint films. Here, we present a VIMP study, complemented by optical microscopy, scanning electron microscopy coupled with X-ray spectrometry (SEM-EDX), nanoindentation-atomic force microscopy (AFM), attenuated total reflectance–Fourier transform infrared spectroscopy (ATR-FTIR), and gas chromatography-mass spectrometry (GC-MS) of the interaction between two blue pigments, indigo

and Prussian blue, and linseed oil in paintings, comparing the results for artificially aged specimens and a painting showing peculiar degradation features.

This multi-technique approach was developed with the aim of providing a broader view, and hence, to attain a deeper understanding of the formation mechanism of the alterations exhibited by the oil painting, *Sant Francesc de Paula*, of anonymous author, 18th century, which is currently included in the painting collection of the Tomàs Balvey Arxiu Museum (Cardedeu, Spain) with reg nº 2258 [31]. As it can be seen in Fig. 1a, the painting surface showed significant chromatic alterations in several light-blue parts of the background painting mainly from the sky, as well as in some of the areas of trees and vegetation. During the conservation treatment and the cleaning process carried out at the *Laboratori de Conservació-restauració de l'Oficina de Patrimoni Cultural de la Diputació de Barcelona*, it was suspected that the darkened layer did not belong to an applied coat of varnish or other resin, but was possibly due to a transformation of the original materials. The painting technique appears to be oil on canvas applied over a thick preparatory red earth layer, following the characteristic techniques used in this period. Vertical fissures and loss of paint indicate that, at some point, the canvas was rolled up, and later on was mounted with cotton lining applied with animal glue onto a wooden stretcher. These vertical fissures were caused by mechanical abrasion removing some of the dark colored superficial layer. The conservation process possibly also included some facing, cleaning and re-varnishing of the surface, although the work was unfinished leaving an irregular surface of decoloration over the blue and green paint layers [32].

Figure 1b,c shows details of the altered and unaltered blue areas of the painting in which samples were taken for the analysis. Our analytical data (vide infra) indicated the presence of a mixture of indigo, Prussian blue and lead white in this light blue area of the sky, thus providing opportunity for studying the possible interactions between these pigments and the organic binder. This study exploits the electroactive character in solid state of both Prussian blue [33–35] and indigo [36–39], whose photochemical degradation has claimed considerable attention [40–43].

2. Experimental

2.1. Instrumentation

A Leica DM2500 P microscope (Leica Microsystems. Heidelberg, Germany) was employed using polarised reflected light at x25 to x400 magnification for the morphological examination of the cross sections prepared from the paint samples. Digital images were acquired using a Leica Digital FireWire Camera (DFC), controlled by the Leica Application Suite (LAS) software.

Morphological examination and elemental analysis of the cross-sections of the paint samples, previously carbon-coated, were performed using a JEOL JSM 6300 scanning electron microscope operating with an Oxford Instruments Link Isis X-ray microanalysis system. The analytical conditions were an accelerating voltage of 20 kV, a beam current of 2×10^{-9} A and a working distance of 15 mm. Qualitative analysis was performed mainly in punctual and area modes. Quantitative microanalysis was carried out using the ZAF

method, which is based on the correction of the matrix effect in multielement analysis that takes place in the simultaneous determination of the concentration of each element present in a multielement material. This theoretical method provides a correction of the X-ray intensity of each element present in the material by means of the application of a series of correction factors for the atomic number effect (which describes the depth of electron penetration and the fraction of electrons that backscatter from the sample), the absorption correction (which describes the absorption of X-rays in the matrix as a function of the composition and depth of electron penetration) and the fluorescence of one elementby the others present). In this study, the counting time was 100 s for major and minor elements. Concentrations were calculated by stoichiometry from element percentages generated by ZAF software used with the Oxford Instruments Link Isis EDX instrument.

Nanoindentation-atomic force microscopy (NI-AFM) is an advanced instrumental technique that allows the determination of the elastic modulus (*EM*) in the microsamples of the original paintings. In this study, a Multimode AFM (Digital Instruments VEECO Methodology Group, USA) with a NanoScope IIa controller was used, which was equipped with a J-type scanner (max. scan size of (150 × 150 × 6) mm). The *EM* of each sample was obtained in the scan asyst peak-force quantitative nanomecanical mode (*QNM*) with a tip Scan Asyst (Bruker) ($k = 3N.m^{-1}$). The *EM* values were calculated by the Bruker Nanoscope 1.40 Analysis software. This process was carried out using the Derjaguin, Muller, Toropov (*DMT*) model [<link rid="bib42">42</link>], The tip radius *R* is calculated by an indirect method using a polystyrene sample with a known *EM* of 2.7 GPa. The indirect method includes the prior determination of deflection by pressing the tip onto a Sapphire disc, and the spring constant of the cantilever by performing a thermal tune. A value of 0.3 was used for the Poisson's ratio. This value is recommended for samples with an *EM* that falls within the 1 GPa < E_s<10 GPa range. *EM* value was collected automatically by the instrument for each pixel of the image. Images with scan sizes of (10 × 10) μm that consisted of 256 lines by pixels, and taken at a scan rate of 0.4–0.5 Hz, were created for each sample during one same scan, which allowed the morphological data in high (2D and 3D) and peak force modes and *EM* to be collected. *EM* was calculated as the average value of the individual *EM* measured in each pixel of an image. At least three images were acquired in each sample. Repeatability was at ca. 5%.

ATR-FTIR spectra of the paint samples and the reconstructed paint films were recorded using a Vertex 70 Fourier-transform infrared spectrometer with an FR-DTGS (fast recovery deuterated triglycine sulphate) temperature-stabilized coated detector and a MKII Golden Gate Attenuated Total Reflectance (ATR) accessory. A total of 32 scans were collected at a resolution of 4 cm^{-1} and the spectra were processed using the OPUS/IR software.

A gas chromatograph Agilent 6890N (Agilent Technologies, Palo Alto, CA, USA) coupled to an Agilent 5973N mass spectrometer (Agilent Technologies) was used for the identification of the binding media of the painting. A capillary column HP-5MS (5% phenyl–95% methylpolysiloxane, 30 m, 0.25 mm i.d., 0.25 μm film thickness, Agilent Technologies) was used to adequately separate components. Polar and non-polar compounds were separately analysed by the hydrolysis procedure, followed by derivatisation with ethyl chloroformate, as described elsewhere [43]. 1.5 μL of the chloroformic solutions of amino acid

or fatty acid derivatives obtained were injected into the GC–MS system in the split mode (split ratio 1:20). Chromatographic conditions for the amino acid derivatives were initial temperature of 100ºC increased with an initial ramp of 5ºC.min^{-1} up to 155ºC and then a final ramp of 15ºC-min^{-1} up to 300ºC held for 10 min. For the fatty acid derivatives the chromatographic conditions were: initial temperature of 50 °C held for 2 min, increased by 20 °C.min^{-1} up to 300 °C and held for 10 min. The helium gas flow was set at 1.3 mL.min^{-1}. Electronic pressure control was set to the constant flow mode with vacuum compensation. Ions were generated by electron ionisation (70 eV). The mass spectrometer was scanned from m/z 20 to m/z 800 in a 1-second cycle time. Mass spectrometer tuning was checked using perfluorotributylamine. EI mass spectra were acquired by the total ion monitoring mode. The interface and source temperatures were 280 °C and 150 °C, respectively. Agilent Chemstation software G1701CA MSD was used for the GC–MS control, peak integration and mass spectra evaluation. Wiley Library of Mass Spectra and NIST were used to identify compounds.

Electrochemical experiments were performed in a three-electrode cell at 298 K using 0.25 M sodium acetate buffer (Panreac) at pH 4.75 as a supporting electrolyte. In order to reproduce the conditions for optional analysis in field, no deaeration of the electrolyte was carried out. A CH I660C potentiostat (Cambria Scientific, Llwynhendy, Llanelli UK) was used. Sample-modified commercial paraffin-impregnated graphite bars (Alpino HB type, 68% wt graphite, diameter 2 mm) were used as working electrodes completing the three-electrode arrangement with a platinum wire counter-electrode and an Ag/AgCl (3 M NaCl) reference electrode. Optionally, semi-derivative convolution of data was carried out in order to enhance peak resolution. Prior to each measurement, the graphite electrode was polished with alumina, rinsed with water and polished by pressing over paper. Then, the electrode was pressed onto the sample deposited on the plane surface of an agate mortar. Sample-modified graphite electrodes were then dipped into the electrochemical cell so that only the lower end of the electrode was in contact with the electrolyte solution.

2.2. Samples and test specimens

Two paint samples from the unaltered light-blue and the altered greenish areas from the sky were taken using a scalpel (Fig. 1b,c). For the optical and scanning electron microscopy studies, both samples were embedded in a transparent polyester resin (Synolite 0328-A-1, DSM Composite Resins AG, Switzerland). Embedded samples were left to set overnight in laboratory conditions (21ºC, 50% R.H) for the polymerization of the resin. Grinding and polishing were carried out using a rotating wet grinder (Labopol 20, Struers, Erkrath, Germany) with different grades of silicon carbide grinding papers (220, 500, 2400) to obtain the corresponding cross-sections.

Reconstructed paint films were prepared by mixing indigo (I), Prussian blue (P) and a 50% wt mixture of indigo and Prussian blue (IP) with linseed oil supplied by (Kremer Pigmente). Pure pigments and their 1:1 mixture were mixed with the appropriate amount of linseed oil until suitable consistence (30% weight composition of pigment) (IO, PO and IPO reconstructed paint specimens). After this the paint was spread

on glass slides in order to form a thin film. The reconstructed paint films were dried and naturally aged at room temperature for 2 years (21ºC, 50% RH). Thickness of the films was in the range 0.3–0.5 mm.

2.3. Accelerated aging tests

Pure pigments and their 50%wt mixture as well as a the reconstructed paint specimens were subjected to UV light exposure by irradiating them in a QUV-Basic chamber with UV lamps UVA-351 nm (Q-Lab Corporation, Cleveland, USA), that emits 25 $W.m^{-2}$ mostly at 300–400 nm, simulating the sunlight spectrum (series UVA). Temperature in the ageing chamber was maintained at constant value of 45 °C. Specimens were exposed to UVA light for 200 h.

3. Results And Discussion

3.1. Optical, scanning electron and atomic force microscopy

Figure 2a shows the image of the sample excised from an altered blue area of the painting. It can be seen that the paint layer exhibits a notable darkening in the surface as consequence of the alteration processes that took place on the painting.

The examination of the cross-section of the altered and unaltered paint samples under the optical microscope allowed the recognition of the layered structure and the morphological features. The stratigraphic distribution of the paint samples examined comprises two light-blue paint layers and two reddish ground layers (Fig. 2b). The upper blue paint layer is thinner (at ca 15 μm) than the lower one (at ca 55 μm) and is composed of blue pigment. In the upper blue paint layer can be seen microparticles and dark-blue aggregates with variable sizes (1–5 μm) of blue pigments. In the inner paint layer can be seen heterometric rounded lead white particles distributed heterogeneously throughout the light-blue microcrystalline matrix. Interestingly, the chromatic alteration observed in the painting is observed in the outer 5 μm of the upper blue paint layer in the cross-section (Fig. 2b), suggesting that the alteration process is a surface phenomenon as confirmed in other studies [19, 44]. The lower red ground layer presents a heterogeneous texture in which translucent, white and red-ochre small grains are dispersed in a reddish matrix and the upper red ground layer shows similar characteristics but a thinner texture. Some other morphological features can be seen in the cross-section, such as microcracks across the paint layers, partial loss of the outer paint layer, cavities between the ground and the paint layers, and a disjunction between both ground layers, which highlight the deterioration of this paint sample.

Backscattered electron (BSE) images and analysis performed by energy dispersive X-ray spectrometry (EDX) on this sample revealed in the lower paint layer well-defined light gray particles (highly scattering) where lead is detected, corresponding to lead white ($2PbCO_3 \cdot Pb(OH)_2$), as can be seen in Fig. 2c. Furthermore, dark-grey (less scattering) amorphous areas and small particles are also identified in the upper paint layer in which iron is detected in significant proportion, along with potassium (Fig. 2d). The

abundance of iron in most part of the upper layer together with potassium suggest the presence of Prussian blue ($Fe^{III}_4[Fe^{II}(CN)_6]_3$ or $KFe^{III}[Fe^{II}(CN)_6].xH_2O$, depending on the preparation procedure). On the other hand, the presence of iron together with aluminium, sulphur and potassium appear to be characteristic of the original method of Prussian blue preparation in which dried blood or another animal matter and alum (aluminium potassium sulphate) as extender are ingredients, following the procedure reported by Woodward [45]. However, in some of these dark grey amorphous areas the absence of iron is evident (results not shown) and this feature could suggest the coexistence of an organic pigment such as indigo, precipitated in alum for shading, and/or a deterioration of the Prussian blue pigment due to a lixiviation of the iron ions/solubilization of the Prussian blue. Finally, ground layers show a typical profile of a red earth pigment due to the identification of aluminum, silicon, magnesium, potassium, calcium and iron (results not shown), but the abundance of lead indicates the possible addition of red lead or the diffusion of lead-compounds (such as lead soaps) from the paint upper layers.

Figure 3 shows the AFM topographic images (10 × 10) μm obtained in samples excised from altered (Fig. 3a) and unaltered (Fig. 3b) areas of the painting. It can be seen that the micromorphology in both cases is similar with pigment grains protruding the surface resulting in Δhigh in the range of 1 μm. It results more interesting the comparison between the elastic modulus obtained for paint samples excised from unaltered and altered areas of the painting which are summarized in Table 1. It is firstly worth of mention that the *EM* values obtained in this research were in the same order as those for the 19th - century oil paintings reported in other studies that focused on changes in nanomechanical properties while aging oil paintings. [46]. The higher values obtained for the *EM* in the altered sample were associated with increased stiffness due to the alteration processes taking place in the painting. As described in sections thereafter, these alteration processes undergone by the painting have resulted in the hydrolysis of the drying oil and the concomitant depolymerisation and loss of the cross-linking of the oil network. Consequently, the paint film has undergone an increase of stiffness.

Table 1
Values of the elastic modulus obtained by means of NI-AFM in microsamples of unaltered and altered paint film excised from the “San Francesc de Paula” painting.

Elastic modulus	Unaltered blue paint (GPa)	Altered blue paint (GPa)
Mean Value	6.9	10.2
Minimum value	6.0	6.3
Maximum value	9.4	20.4

3.2. FTIR spectroscopy

The results of the FTIR analysis of the altered paint sample (Fig. 4) evidenced the predominance of absorption bands ascribed to lead carbonate in the basic or hidrocerussite form ($2PbCO_3.Pb(OH)_2$)

(absorption bands at 3536, 1393, 1045 and 679 cm^{-1}). On the other hand, the absorption bands appearing in the region between 3000 – 2900 cm^{-1} are related to stretching vibrations of methyl and methylene groups from fatty acid chains, demonstrating the presence of an organic material of lipidic type as binding media. This organic material exhibits an advanced state of degradation, as confirmed by the identification of a carboxylic acid band related to the free fatty acids at about 1703 cm^{-1}, as well as by the spectral region between 1650 – 1500 cm^{-1}, with characteristic bands attributed to metal carboxylates, mainly lead carboxylates (band at 1506 and shoulder at 1537 cm^{-1}) formed between the free fatty acids and the lead ions of the pigment, and oxalates of calcium (weddellite and whewellite at 1643 and 1620 cm^{-1}) and lead (1651 cm^{-1}) [14]. In this sense, it should be pointed out that calcium oxalates are more abundant in the altered paint sample than in the unaltered one (results not shown) and these compounds can contribute to the chromatic alterations showed in the painting. Other inorganic compounds were also identified in the infrared spectrum such as calcite ($CaCO_3$: 1400, 871 cm^{-1}), siliceous minerals ascribed to earth pigments (1166, 1026, 797 and 767 cm^{-1}) and alum (1094 cm^{-1}).

A low intensity absorption band with a maximum at 2089 cm^{-1} related to the stretching vibration of CN group confirms the presence of Prussian blue in accordance with the results of SEM/EDX. The broadening of this band and the shoulder at 2050 cm^{-1} suggest the coexistence of different species with variated oxidation states formed through redox reactions of this pigment [47]. However, the considerable overlap between the absorption bands of the organic and inorganic compounds present in the pain samples due to the complexity of this matrix make difficult the confirmation of the coexistence of other pigments such as indigo.

Figure 5 shows the IR absorption spectra of the reconstructed pain specimens made with Prussian blue (PO) (Fig. 5a), indigo (IO) (Fig. 5b) and the mixture 1:1 indigo-Prussian (IPO) (Fig. 5c). The IR spectrum of Prussian blue + oil paint film is dominated by strong band at 2082 cm^{-1} ascribed to the stretching vibration of CN group. Indigo + oil paint film exhibits abundant IR bands in the fingerprint region dominated by the band at 1069 cm^{-1} and moderate bands at 1625 and 1610 cm^{-1} ascribed to the stretching vibration of C = O group in indigoid molecules present in natural indigo. Linseed oil is recognized in both IR spectra by sharp bands at 2924 and 2853 cm^{-1} associated with the stretching vibrations of methyl and methylene groups in triacylglycerol molecules and by the band at 1738 cm^{-1} ascribed to the carbonyl bond in the ester groups of triacylglycerol molecules. The IR spectrum of the indigo-Prussian blue + oil reconstructed paint film is a combination of the IR spectra of both pigments plus the drying oil. This last spectrum is dominated by the Prussian blue band of CN groups at 2082 cm^{-1}. Moderate bands of carbonyl stretch at 1738 cm^{-1} and C-O stretch vibrations at 1240, 1158 and 1097 cm^{-1} ascribed to the linseed oil are also present. Interestingly a shoulder at 1705 cm^{-1}, ascribed to stretching vibrations of free fatty acids released by the hydrolysis reaction undergone by the triacylglycerol molecules of the linseed oil is exclusively observed in reconstructed paint films containing Prussian blue.

Figure 6a shows the IR spectra of the indigo-Prussian blue + oil reconstructed paint film (IPO) (IR spectrum a) after ageing and the reconstructed paint films (IPO-N, IPO-UVA) after natural (IR spectrum b) and UV solar light (IR spectrum c). It can be recognized changes in spectral region I (1800 – 1600 cm^{-1}) and spectral region II (1100 – 1000 cm^{-1}). These changes in IR bands can be seen in detail in Fig. 6b. Interestingly a new band at 1610 cm^{-1} ascribed to carbonyl band in indigoid molecules as well as a new band at 1073 cm^{-1} ascribed to stretching vibrations of OH groups occurs in both natural and UV solar light aged paint films.

3.3 Gas chromatography-mass spectrometry

With the purpose of completely characterizing the organic material used as binding media in the painting, and thus, complementing the results obtained by ATR-FTIR, representative fragments of the altered and unaltered paint samples were analyzed by means of GC-MS. In Fig. 7 is shown the chromatogram obtained for the altered paint sample that revealed the presence of monocarboxylic even-numbered saturated fatty acids (peaks 4–5) containing 16 and 18 carbon atoms, with stearic acid (18:0) as the most abundant, and short-chain dicarboxylic acids with 8, 9 and 10 carbon atoms (peaks 1–3) in a significant proportion formed due to oxidation process undergone by the unsaturated fatty acids (oleic, linoleic and linolenic). A similar chromatographic profile was obtained for the paint sample from the unaltered area (results not shown).

The occurrence of these compounds confirms the presence of an organic material of lipid type as binder. On the other hand, taken into account these results, the P/S ratio (chromatographic peak area of palmitic acid versus chromatographic peak area of stearic acid) obtained is 0.6–0.7, which is not adjusted for the expected values for linseed, walnut, poppy or mixtures of them, commonly used in oil paintings [48]. This deviation indicates significant variations in the content of fatty acids constituent of the drying oil as a consequence of the high degree of degradation of the binding media, which has undergone an extensive hydrolysis process and the subsequent formation of metal soaps between the free-fatty acids of the oil and the metal ions of the pigments, as well as oxalates, as shown in the results obtained by the ATR-FTIR analysis.

3.4. Voltammetric pattern

Figure 8 shows the square wave voltammograms of microparticulate deposits of a) indigo and b) isatin abrasively transferred onto the surface of graphite electrodes in contact with 0.25 M HAc/NaAc aqueous buffer at pH 4.75. These are accompanied by the voltammograms corresponding to c) unaltered and d) altered layers of the *Sant Francesc de Paula* paint. Upon scanning the potential in the negative direction, indigo (Fig. 8a) displays two well-defined peaks at −0.30 (I) and 0.45 V vs. Ag/AgCl (II) corresponding, respectively, to the reduction of indigo (IND) to leucoindigo (LEU) and the oxidation of indigo to dehydroindigo (DHI). These two proton-assisted solid-state processes are summarized in Scheme 1 and can be represented as [36–38]:

$$\{IND\}_{solid} + 2H^{+}_{aq} + 2e^{-} \rightarrow \{LEU\}_{solid} \quad (1)$$

$\{IND\}_{solid} \rightarrow \{DHI\}_{solid} + 2H^{+}_{aq} + 2e^{-}$ (2)

In turn, isatin produces a unique, intense cathodic peak at ca. −0.70 V (III) (Fig. 8b), corresponding to the proton-assisted reduction to hydroxylated derivatives (see scheme 1) [39, 49].

The unaltered blue submicrosample (Fig. 8c) yields the indigo-localized peaks I and II accompanied by broad peaks at −0.15 (IV) and 0.80 V (V), which can be unambiguously attributed to Prussian blue centered processes on the basis of abundant literature on the electrochemistry of this compound [33–35] and our blank experiments in synthetic specimens (*vide infra*). These processes correspond, respectively, to the reduction of Fe(II) centers and the oxidation of Fe(III) ones coupled to the entrance/issue of electrolyte charge-balancing cations [33–35]. Signals attributable to lead white were recorded only in positive-going voltammograms appearing as weak anodic signals at ca. −0.50 V, in agreement with prior studies [50, 51]. The voltammetric peaks IV and V can be represented as [33–35]:

$KFe^{III}[Fe^{II}(CN)_6]_{solid} + K^{+}_{aq} + e^{-} \rightarrow K_2Fe^{II}[Fe^{II}(CN)_6]_{solid}$ (3)

$KFe^{III}[Fe^{II}(CN)_6]_{solid} \rightarrow Fe^{III}[Fe^{III}(CN)_6]_{solid} + K^{+}_{aq} + e^{-}$ (4)

Interestingly, the voltammograms of submicrosamples extracted from the altered regions of the paint show intense signals III and IV while the indigo signals and the Prussian blue signal V vanish (Fig. 8d). These features suggest that there is an oxidation of indigo to isatin and Prussian blue to Berlin green responsible for the chromatic change of the paint.

3.5. Degradation pathways

In order to study the possible mechanisms of degradation, specimens of indigo, Prussian blue, 50%wt mixture of these pigments and reconstructed model paint films containing either indigo, Prussian blue, 50%wt mixture of these pigments dispersed into linseed oil (see experimental section), were submitted to two aging protocols, natural ageing for 2 years and accelerated ageing with UVA (UV solar light) for 200 h. The most relevant voltammetric features are summarized in Figs. 9 and 10. The former superimposes the negative-going potential scan voltammograms of indigo, Prussian blue and o 50% wt mixture of both components, clearly showing the indigo-centered signals I and II and the Prussian blue centered peaks IV and V.

In Fig. 10a, the electrochemical response of the parent pigment blue mixture is superimposed to those of the mixture submitted to natural and UV aging, while Fig. 10b compares the voltammograms of a paint film specimen and those submitted to natural and UV solar light aging. The voltammetric features of pigments and paint specimens after natural and UV solar light aging were essentially identical. The most relevant features can be summarized as:

a) In the pure pigments, as well as in the pigment mixtures, natural aging determines a decrease of the indigo signal II without concomitant decrease of the signal I, a light increase in the Prussian blue signal IV without variation of the signal V, all these features being accompanied by the appearance of a new

voltammetric peak at 1.05 V (VI). Upon natural and UV solar light aging, the decrease of the indigo signal becomes more pronounced while the peak VI becomes clearly enhanced. This last signal can tentatively be attributed to a species resulting from the hydroxyl addition to the indigo molecule (see Scheme 1) whose electrochemical oxidation should occur at high potentials.

b) The paint oil specimens show the Prussian blue signal V clearly depleted relative to the indigo signals. Natural aging determines the same features described for the pure pigments, but here the Prussian blue signals become enhanced. Under UV aging, the peak VI is considerably enhanced whereas both indigo peaks I and II are depleted.

c) In all indigo-containing specimens, the isatin signature (peak III) appears upon aging, being particularly enhanced when UV aging was employed.

These voltammetric data are consistent with infrared features. As can be seen in Fig. 5b, appearance of a new stretch band of C = O groups in indigoid molecules at 1605 cm^{-1} on UV and UV solar light ageing suggests diversification of indigoid molecules on ageing. Similarly, the new indigo IR band at 1073 cm^{-1}, which has been tentatively ascribed to OH groups, also suggests a diversification of indigoid molecules as result of the alteration processes that have taken place. Appearance of the carbonyl signal at 1705 cm^{-1} only in reconstructed paint films that contain Prussian blue (PO and IPO), suggests that the hydrolysis process undergone by the linseed oil is promoted by the Prussian blue pigment.

These features can be interpreted on the basis of studies on the degradation of indigo and Prussian blue pigments. In regard to indigo, its degradation is in principle promoted by oxidants [41], the degradation by light being, however, particularly intense [42]. According to Iuga et al. [43], there are two (main) indigo degradation pathways catalyzed by hydroxyl (•OH) and hydroperoxyl (•OOH) radicals. In turn, the hydroxyl-catalyzed degradation can lead to dehydroindigo via intermediate formation of an indigo radical anion after proton abstraction, or via OH addition to the central C = = C indigo bond. Ultimately, indigo photodegradation yields isatin, isatoic anhydride and anthranilic acid [41–43, 52] whereas indigo degradation by ozone yields isatin and isatoic anhydride [53].

In regard to Prussian blue, Samain et al. [20] have reported that it can be partially oxidized to Berlin green $(KFe^{III}[Fe^{II}(CN)_6])_x(Fe^{III}[Fe^{III}(CN)_6])_{1-x}$. The degradation process appears to be facilitated in the presence of linseed oil binder and lead white, leading to the reduction of Prussian blue to Berlin white, $K_2Fe^{II}(Fe^{II}(CN)_6$, at the exposed paint surface and an oxidation to Berlin green in the bulk of the paint layer [20]. Then, the combination of isatin and other indigo degradation products and Berlin green can be responsible for the observed chromatic alteration in the *Sant Francesc de Paula* painting.

On the other hand, the polymerization of drying oils produces free radicals (alcoxyle, •OR, peroxyle, •OOR) derived from hydroperoxides [21], able to promote the above oxidation reactions. Accordingly, the formation of isatin, and hence, the orange-brownish hue acquired by the degraded zones of the *Sant Frances de Paula* paint, can be attributed to the oxidation of indigo promoted by free radicals generated

in the oil binding. As previously noted, this situation is mainly reproduced in paint specimens prepared from indigo without Prussian blue. To interpret the minor presence or even the absence of isatin in aged specimens containing both Prussian blue and indigo can be rationalized on considering the peculiar characteristics of the interaction of Prussian blue with reactive oxygen species (ROS). This compound acts as catalyst for H_2O_2 reduction under electrochemical conditions [54, 55] where it appears to be partially dissolved releasing Fe^{2+} (aq) and ferrocyanide associated to local production of HO^-, so that Fe^{2+} (aq) ions initiate the Fenton reaction with H_2O_2 generating hydroxyl radicals [56]. On the contrary, it has been reported that under 'chemical' conditions, Prussian blue nanoparticles act as radical scavengers, in particular abstracting •OH radicals mimicking the activity of peroxidases [57, 58].

On the basis of the foregoing set of considerations, the different degradation pathways observed in synthetic paint film specimens and localized areas of the *Sant Francesc de Paula* paint can be interpreted taking into account that the grain size and the nature of the local binding environment can affect significantly the stability of the pigments [52, 59]. Under 'ordinary' conditions of degradation, as is the case of the prepared paint film specimens, Prussian blue which exerts an effect of moderator, acting as radical scavenger [57, 58], being slowly oxidized to Berlin green and leading indigo degradation to the formation of adducts with the radicals, as schematically depicted in Scheme 1.

In the case of the *Sant Francesc de Paula* paint, since the canvas was rolled up and re-mounted onto a wooden stretcher and subsequently re-varnished [32], the produced fissures provided opportunity for a reinforced action of light and humidity on the pigment layers. Here, Prussian blue acts as an initiator of the Fenton reaction [56] rather than a radical scavenger and promotes the oxidation of indigo to isatin. This process formally results from the reaction of indigo with O_2, or, possibly, with H_2O_2 formed, in the absence of radical scavenging, by condensation of hydroxyl radicals. Scheme 2 shows an idealized scheme of the possible processes involved in pigment degradation.

4. Conclusions

The degradation of oil paints containing indigo and Prussian blue pigments has been studied by solid state electrochemistry aided by optical, scanning electron and atomic-force microscopies, SEM-EDX, ATR-FTIR and CG-MS. Voltammetry of immobilized particles data on sub-microsamples from synthetic oil paint specimens and samples from the *Sant Francesc de Paula* painting from the museum of Cardedeu permit to detect the presence of isatin and Berlin green in highly degraded areas of the paint, resulting in a significant chromatic fit respect to unaltered light-blue areas.

Voltammetric data on samples from paint specimens submitted to natural, UV and UV solar light aging can be interpreted on the basis of a dual reaction scheme in which the action of ROS produced in the binding media interact with indigo and Prussian blue. Under 'ordinary' conditions, this compound acts as a selective radical scavenger determining the preferential addition of ROS to the C = C central bond of indigo. Under drastic conditions of degradation, as is the case of localized areas of the *Sant Francesc de Paula* painting, Prussian blue acts as an oxidation promoter of the indigo oxidation to isatin. Conjointly

considered, the reported data illustrate the capabilities of the voltammetry of immobilized particles to acquire information on complex systems.

Declarations

Ackonwledgements: Financial support from the MINECO Project CTQ2017-85317-C2-1-P which is supported with *Ministerio de Economía, Industria y Competitividad* (MINECO) and *Fondo Europeo de Desarrollo Regional* (ERDF) funds is gratefully acknowledged. The authors wish to thank Teresa Blanch Bofill, director of the Museu Arxiu Tomàs Balvey de Cardedeu (MATBC, Barcelona) for generous access to the painting and for organizing the *Jornada d'estudi de la pintura de Sant Francesc de Paula* to discuss the results of the research conducted by GRAPAC-CETEC Patrimoni de la UAB-IQS/URL, Institut Universitari de Restauració del Patrimoni (IRP) de la Universitat Politècnica de València (UPV) and Universitat de València (UV), and to the Oficina de Patrimoni Cultural de la Diputació de Barcelona in which Conservation Programme the intervention of the painting and preliminary studies were technically and financially supported.

Funding: MINECO Project CTQ2017-85317-C2-1-P which is supported with Ministerio de Economía, Industria y Competitividad (MINECO) and Fondo Europeo de Desarrollo Regional (ERDF).

Declarations: None of the authors have any competing interest in the manuscript.

Authors' contribution: ADC: design and coordination of the study and modeling electrochemical data; MTDC: performance of laboratory specimens, AFM-nanoindentation and design and coordination of the study and interpretation of AFM-indentation, infrared and SEM-EDX data; LOC: performance of accelerated ageing of specimens, morphological analysis of paint samples using optical and Scanning Electron Microscopy, SEM-EDX, GC-MS and FTIR analysis and data interpretation; MD: performance and interpretation of voltammetric data; NGF: analysis chemical and mineralogic using light microscopy and SEM-EDX and participation in data interpretation; RGF: preliminary studies, diagnosis and conservation treatment of the painting; MAI: stratigraphic description and analysis mineralogic using light microscopy and participation in data interpretation.

References

1. Matteini M, Moles A. La Chimica nel Restauro. Firenze: Nardini; 1989.
2. Mills JS, White R. The Organic Chemistry of Museum Objects. London: Buttersworth; 1994.
3. Berrie BH, Strumfels Y. Change is permanent: thoughts on the fading of cochineal-based watercolor pigments. Herit Sci. 2017;5:5–30.
4. Erhardt D, Tumosa CS, Mecklenburg MF. Long-term chemical and physical processes in oil paint films. Stud Conservat. 2005;50:143–50.
5. Meilunas RJ, Bentsen JG, Steinberg A. Analysis of aged paint binders by FTIR Spectroscopy. Stud Conserv. 1990;35:33–51.

6. Mallégol J, Lemaire J, Gardette JL. Drier influence on the curing of linseed oil. Progr Org Coat. 2009;39:107–13.
7. Breitbach AM, Rocha JC, Gaylarde CC. Influence of pigment on biodeterioration of acrylic paint films in Southern Brazil. J Coat Technol Res. 2011;8:619–28.
8. Robinet L, Corbeil MC. The characterization of metal soaps. Stud Conserv. 2003;48:23–40.
9. Plater MJ, De Silva B, Gelbrich T, Hursthouse MB, Higgitt CL, Saunders DR. The characterization of lead fatty acid soaps in “protusions” in aged traditional oil paint”. Polyhedron. 2003;22:3171–79.
10. Cotte M, Checroun E, Susini J, Dumas P, Tchoereloff P, Bernard M, Walter P. Kinetics of oil saponification by lead salts in ancient preparations of pharmaceutical lead plasters and painting lead mediums. Talanta. 2006;70:1136–42.
11. Mazzeo R, Prati S, Quaranta M, Joseph E, Kendix E, Galeotti M. Attenuated total reflection micro FTIR characterization of pigment-binder interaction in reconstructed paint films. Anal Bioanal Chem. 2008;392:65–76.
12. Keune K, van Loon A, Boon JJ. SEM Backscattered-Electron images of paint cross sections as information source for the presence of the lead white pigment and lead-related degradation and migration phenomena in oil paintings. Micros Microanal. 2011;22:448–57.
13. Kuene K, Boon JJ. Analytical imaging studies of Saint cross-sections illustrate the oil paint defect of lead soap aggregate formation. Stud Conserv. 2007;52:161–76.
14. Salvadó N, Butí S, Nicholson J, Emerich H, Labrador A, Pradell T. Identification of reaction compounds in micrometric layers from gothic paintings using combined SR-XRD and SR-FTIR. Talanta. 2009;79:419–28.
15. Genestar C, Pons C. Earth pigments in painting: characterization and differentiation by means FTIR spectroscopy. Anal Bioanal Chem. 2005;382:269–74.
16. Casanova-González E, García-Bucio A, Ruvalcaba-Sil JL, Santos-Vasquez V, Esquivel B, Falcón T, Arroyo E, Zetina S, Roldán ML, Domingo C. Surface-enhanced Raman spectroscopy spectra of Mexican dyestuffs. J Raman Spectrosc. 2012;43:1551–59.
17. Higgitt C, Spring M, Saunders D. Pigment-medium interactions in oil paint films containing red lead or lead-tin yellow. Natl Gallery Tech Bull. 2003;24:75–96.
18. Kuene K, Van Loon A, Boon JJ. SEM backscatteredelectron images of paint cross-sections as information source for the presence of the lead white pigment and lead-related degradation and migration phenomena in oil paintings. Microsc Microanal. 2011;17:696–701.
19. Kirby J, Saunders D. Fading and colour Change of Prussian blue: Methods of Manufacture and the Influence of extenders. The National Gallery Technical Bulletin. 2004;25:73–99.
20. Samain L, Gilbert B, Grandjean F, Long GJ, Strivay D. Redox reactions in Prussian blue containing paint layers as a result of light exposure. J Anal Atom Spectrom. 2013;28:524–35.
21. Weerd J, Van Der Loon A, Boon JJ. FTIR Studies of the Effects of Pigments on the Aging of Oil. Stud Conservat. 2005;50:3–22.

22. Cotte M, Checroun E, De Nolf W, Taniguchi Y, De Viguerie L, Burghammer M, Walter P, Rivard C, Salomé M, Janssens K, Susini J. Lead soaps in paintings: Friends or foes? Stud Conservat. 2017;62:2–23.
23. Scholz F, Meyer B. Voltammetry of solid microparticles immobilized on electrode surfaces. Electroanal Chem. 1998;20:1–86.
24. Scholz F, Schröder U, Gulabowski R, Doménech-Carbó A. Electrochemistry of Immobilized Particles and Droplets, 2nd edit. Berlin-Heidelberg: Springer; 2014.
25. Doménech-Carbó A, Labuda J, Scholz F. Electroanalytical chemistry for the analysis of solids: characterization and classification (IUPAC Technical Report). Pure Appl Chem. 2013;85:609–631.
26. Doménech-Carbó A, Doménech-Carbó MT, Costa V. Electrochemical Methods for Archaeometry, Conservation and Restoration (Monographs in Electrochemistry Series Scholz F Edit). Berlin-Heidelberg: Springer; 2009.
27. Doménech-Carbó A. Electrochemistry for conservation science. J Solid State Electrochem. 2010;14:349–51.
28. Doménech-Carbó A, Doménech-Carbó MT. Electroanalytical techniques in archaeological and art conservation. Pure Appl Chem. 2018;90:447–62.
29. Ortiz-Miranda AS, Doménech-Carbó A, Doménech-Carbó MT, Osete-Cortina L, Bolívar-Galiano FF, Martín-Sánchez I, López-Miras MM. Electrochemical characterization of biodeterioration of paint films containing cadmium yellow pigment. J Solid State Electrochem. 2016;20:3287–302.
30. Ortiz-Miranda AS, Doménech-Carbó A, Doménech-Carbó MT, Osete-Cortina L, Bolívar-Galiano FF, Martín-Sánchez I. Analyzing chemical changes in verdigris pictorial specimens upon bacteria and fungi biodeterioration using voltammetry of microparticles. Herit Sci. 2017;5:8.
31. VVAA. “Sant Francesc de Paula”. Anàlisi d’una restauració in Jornada tècnica sobre la restauració de l’obra pictòrica de Sant Francesv [Francesc] de Paula, 16 juny. Barcelona: Cardedeu; 2017.
32. Gasol R. Memòria de la conservació-restauració del quadre “Sant Francesc de Paula” (Núm. In: Reg. 2258) del Museu Arxiu Tomàs Balvey de Cardedeu. Barcelona: Oficina de Patrimoni Cultural de la Diputació de Barcelona; 2016.
33. Scholz F, Dostal A. The formal potentials of the solid metal hexacyanometalates. Angew Chem Int Ed. 1995;34:2685–87.
34. Dostal A, Meyer B, Scholz F, Schröder U, Bond AM, Marken F, Shaw SJ. Electrochemical study of microcrystalline solid prussian blue particles mechanically attached to graphite and gold electrodes: electrochemically induced lattice reconstruction. J Phys Chem. 1995;99:2096–103.
35. Dostal A, Kauschka G, Reddy SJ, Scholz F. Lattice contractions and expansions which accompany the electrochemical conversion of Prussian blue and the reversible and irreversible insertion of rubidium and thallium ions. J Electroanal Chem. 1996;406:155–63.
36. Bond AM, Marken F, Hill E, Compton RG, Hügel H. The electrochemical reduction of indigo dissolved in organic solvents and as a solid mechanically attached to a basal plane pyrolytic graphite electrode immersed in aqueous electrolyte solution. J Chem Soc Perkin Trans. 1997;2:1735–42.

37. Komorsky-Lovric S, Mircevski V, Scholz F. Voltammetry of organic microparticles. Mikrochim Acta. 1999;132:67–77.
38. Doménech-Carbó A, Doménech-Carbó MT, Vázquez De Agredos-Pascual ML. Dehydroindigo: a New Piece into the Maya Blue Puzzle from the Voltammetry of Microparticles Approach. J Phys Chem B 2006;110:6027 – 39.
39. Doménech-Carbó A, Doménech-Carbó MT, Vázquez De Agredos-Pascual ML. Electrochemical monitoring Maya Blue preparation from Maya's ancient procedures. J Solid State Electrochem 2007;11:1335 – 46.
40. Grosjean D, Whitmore PM, Cass GR. Ozone fading of natural organic colorants - mechanisms and products of the reaction of ozone with indigos. Envir Sci Technol. 1988;22:292–98.
41. Novotná P, Boon JJ, van der Horst J. Pacákova V Photodegradation of indigo in dichloro-methane solution. Color Technol. 2003;119:121–27.
42. Yamazaki S, Sobolewski AL, Domcke W. Molecular mechanisms of the photostability of indigo. PhysChemChemPhys 2011;13:1618–28.
43. Iuga C, Ortíz E, Alvarez-Idaboy JR, Vivier-Bunge A. Molecular description of indigo oxidation mechanisms initiated by OH and OOH radicals. J Phys Chem A. 2012;116:3643–651.
44. Derjaguin BV, Muller VM, Toropov Yu P. Effect of contact deformations on the adhesion of particles. J Colloid Interface Sci. 1975;53:314–26.
45. Woodward J. Praeparato caeruli Prussiaci ex Germania missa ad Johannem Woodward. Philosophical Transactions. XXXIII, nº. 381, January-February 1724, pp. 15–17.
46. Salvant J, Barthel E, Menu M. Nanoindentation and the micromechanics of Van Gogh oil paints, hal-00593798, 2011. Available: http://hal.archives-ouvertes.fr. [Accessed: 02/04/2020].
47. Christensen PA, Hamnett A, Higgins SJ. A study of electrochemically grown Prussian blue films using Fourier-transform infrared spectroscopy. J Chem Soc Dalton Trans 1990; 2233–8.
48. Doménech-Carbó MT, Casas-Catalán MJ, Doménech-Carbó A, Mateo-Castro R, Gimeno-Adelantado JV, Bosch-Reig F. Analytical study of canvas painting collection from the Basilica de la Virgen de los Desamparados using SEM/EDX, FT-IR, GC and electrochemical techniques. Fresenius J Anal Chem. 2001;369:571–75.
49. Diculescu VC, Kumbhat S, Oliveira-Brett AM. Electrochemical behaviour of isatin at a glassy carbon electrode. Anal Chim Acta. 2006;575:190–7.
50. Doménech-Carbó A, Doménech-Carbó MT, Mas-Barberá X. Identification of lead pigments in nanosamples from ancient paintings and polychromed sculptures using voltammetry of nanoparticles/atomic force microscopy. Talanta. 2007;71:1569–79.
51. Doménech-Carbó A, Doménech-Carbó MT, Peiró-Ronda MA. 'One-touch' voltammetry of microparticles for the identification of corrosion products in archaeological lead. Electroanalysis. 2011;23:1391–400.

52. Castañeda Delgado M. El índigo en la pintura de caballete novohispana: mecanismos de deterioro. Intervención. 2019;1:25–35.
53. Ben Hmida S, Ladhari N. Study of Parameters Affecting Dry and Wet Ozone Bleaching of Denim Fabric. Ozone Sci Eng. 2015;38:175–80.
54. Chumming P, Xianqing J. Electrochemical synthesis of Fe_3O_4-PB nanoparticles with core-shell structure and its electrocatalytic reduction toward H_2O_2. J Solid State Electrochem. 2009;13:1273–78.
55. Prabhu P, Suresh Babu R, Sriman Narayanan S. Synergetic effect of Prussian blue film with gold nanoparticle graphite-wax composite electrode for the enzyme-free ultrasensitive hydrogen peroxide sensor. J Solid State Electrochem. 2014;18:883–91.
56. Noël J-M, Médard J, Combellas C, Kanoufi F. Prussian Blue Degradation during Hydrogen Peroxide Reduction: A Scanning Electrochemical Study on the Role of the Hydroxide Ion and Hydroxyl Radical. ChemElectroChem. 2016;3:1178–84.
57. Zhang W, Hu S, Yin JJ, He W, Lu W, Ma W, Gu N, Zhang Y. Prussian Blue Nanoparticles as Multienzyme Mimetics and Reactive Oxygen Species Scavenger. J Am Chem Soc. 2016;138:5860–65.
58. Chen J, Wnag Q, Huang L, Zhang H, Rong K, Zhang H, Dong S. Prussian blue with intrinsic heme-like structure as peroxidase mimic. Nano Res. 2018;11:4905–13.
59. Mills JS, White R. The Organic chemistry of museum objects. Oxford: Butterworth-Heinemann; 1994.

Figures

Figure 1

Photograph of the “Sant Francesc de Paula” painting (a). The arrows mark the points were the paint samples were taken from altered (b) and unaltered (c) areas.

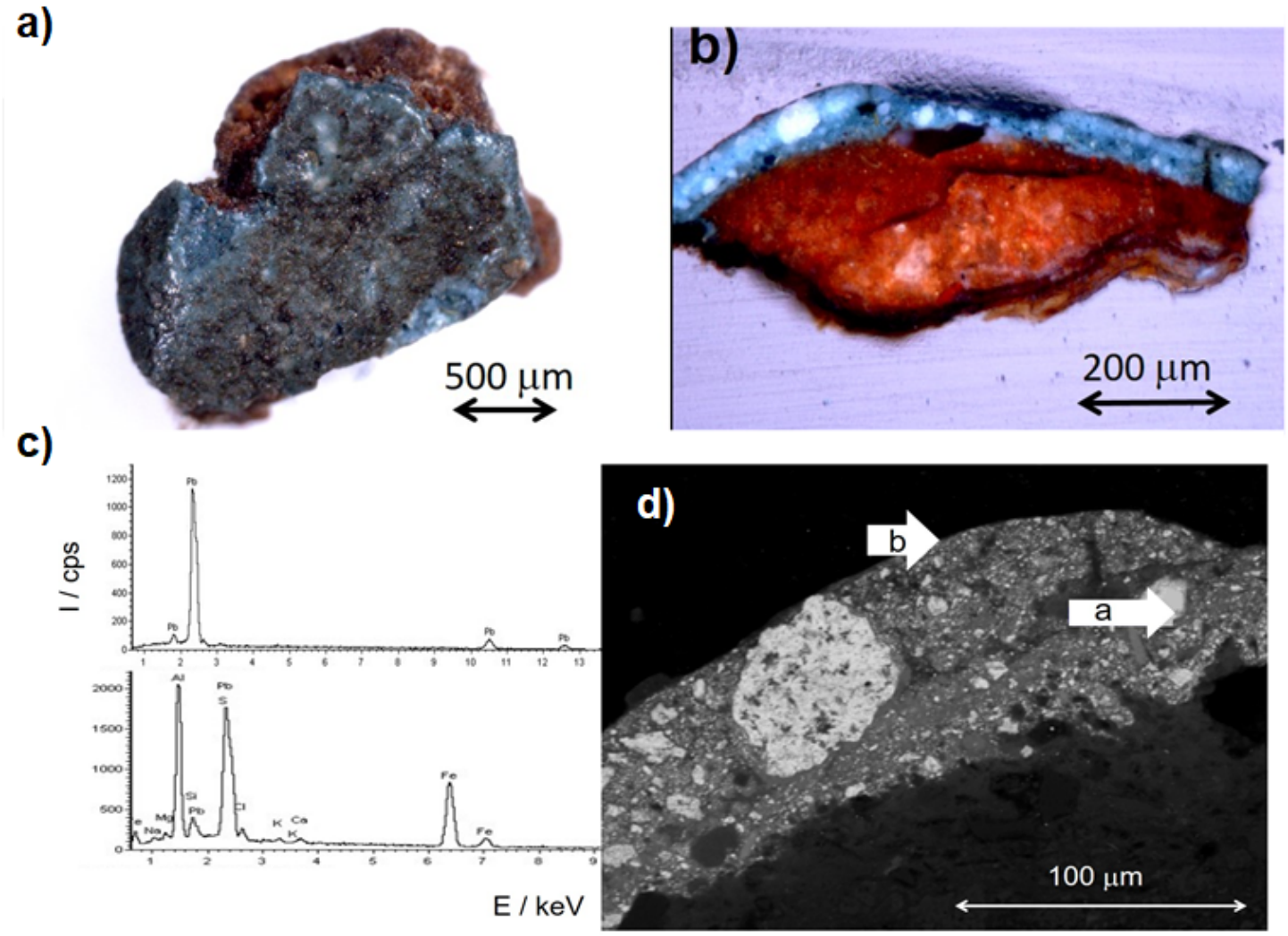

Figure 2

a) Microphotograph of the sample from the blue altered paint; b) microphotograph of the cross section of the sample from the blue altered paint; c,d) FESEM-EDX analyses performed in the altered sample of Figure 1: c) X-ray spectra acquired in a white grain of lead white located in the lower paint layer (upper) and in a blue area located in the lower paint layer (below); d) backscattered electron image of the the cross-section of the sample.

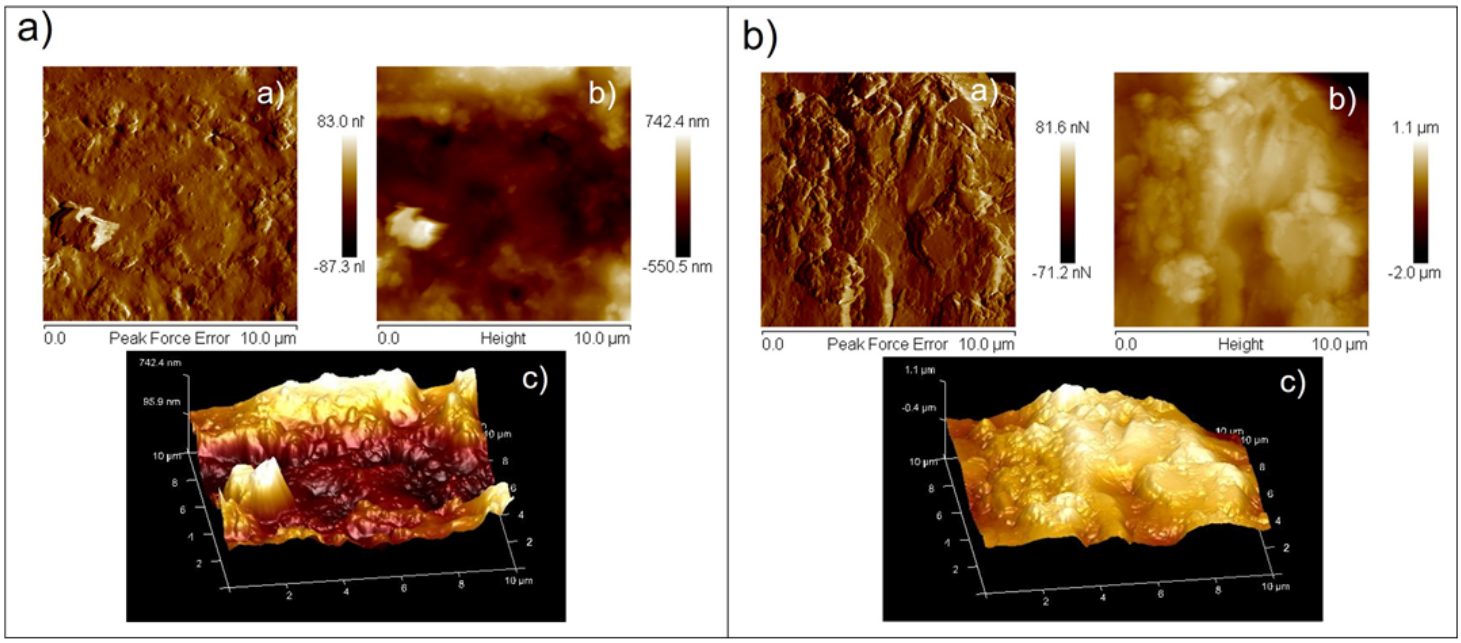

Figure 3

a) sample from blue altered paint (X and Y scale bar = 10 µm, Z = 742.4 nm); b) sample from blue unaltered paint (X and Y scale bar = 10 µm, Z = 1.1 µm). For both samples is shown AFM topographic images in: a) peak force amplitude mode; b) peak force height mode; c) height 3D map.

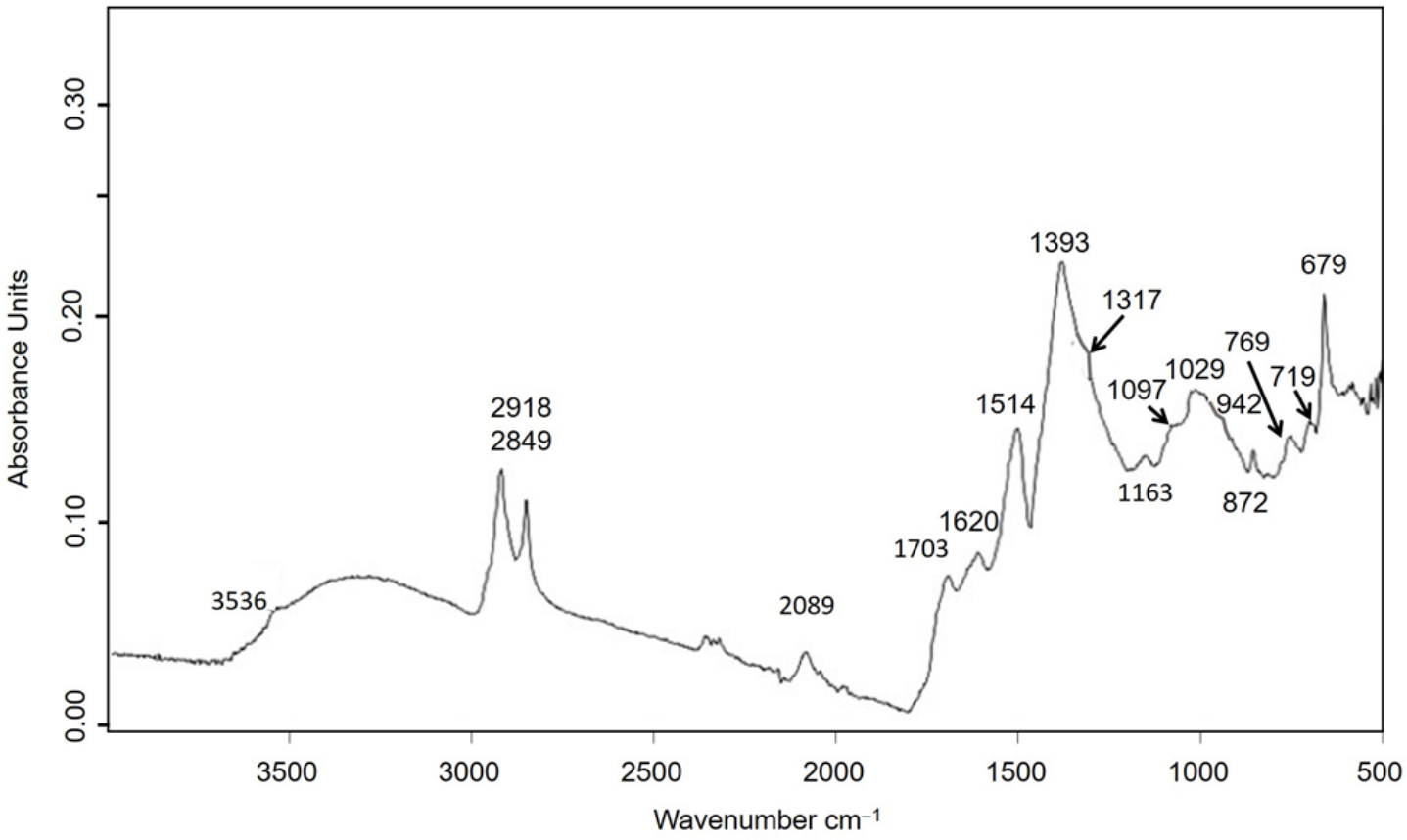

Figure 4

IR absorption spectra of the paint layer of the altered pain sample.

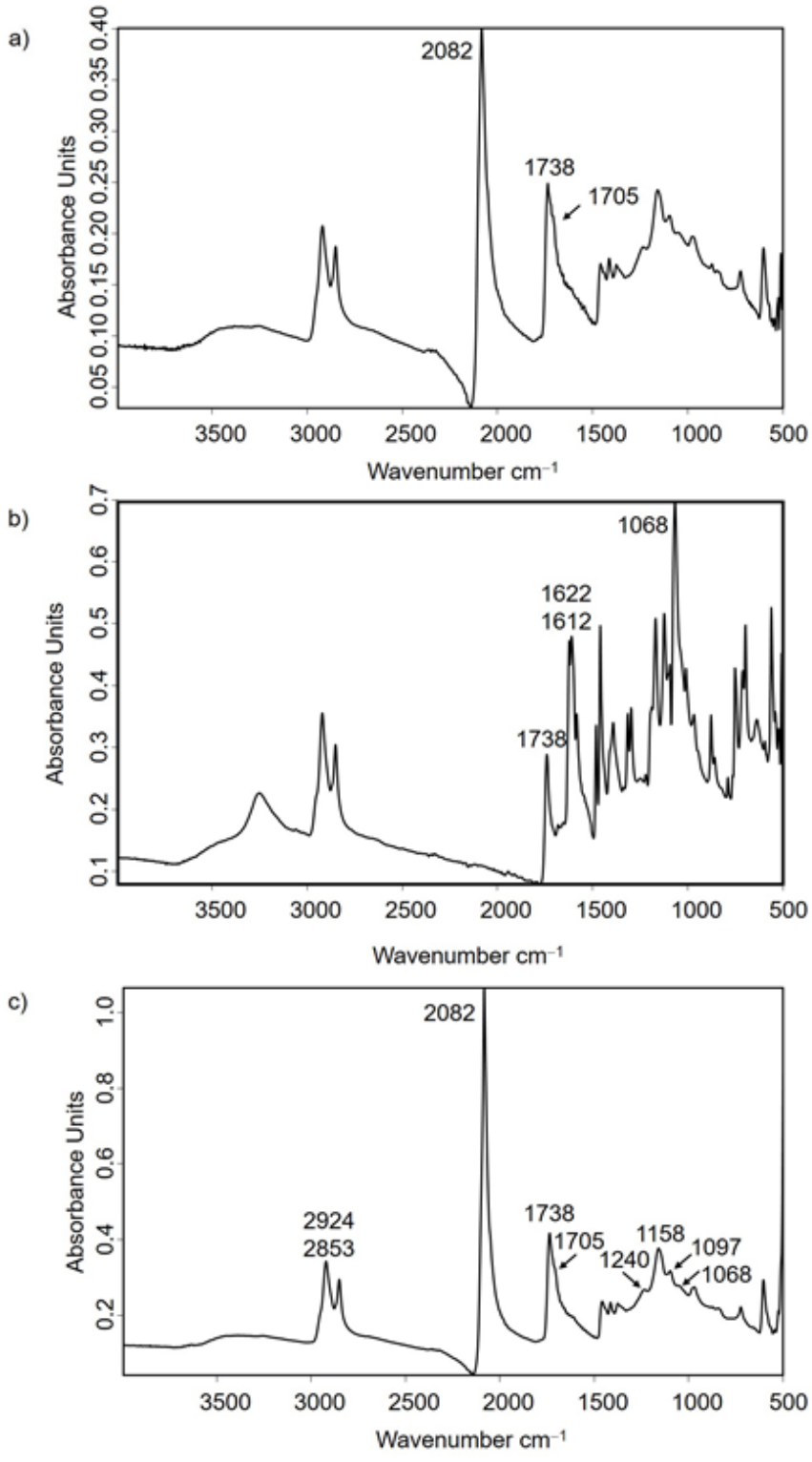

Figure 5

IR absorption spectra of: a) Prussian blue+linseed oil (PO); b) Indigo+linseed oil (IO); c) Prussian blue+indigo+linseed oil paint film (IPO).

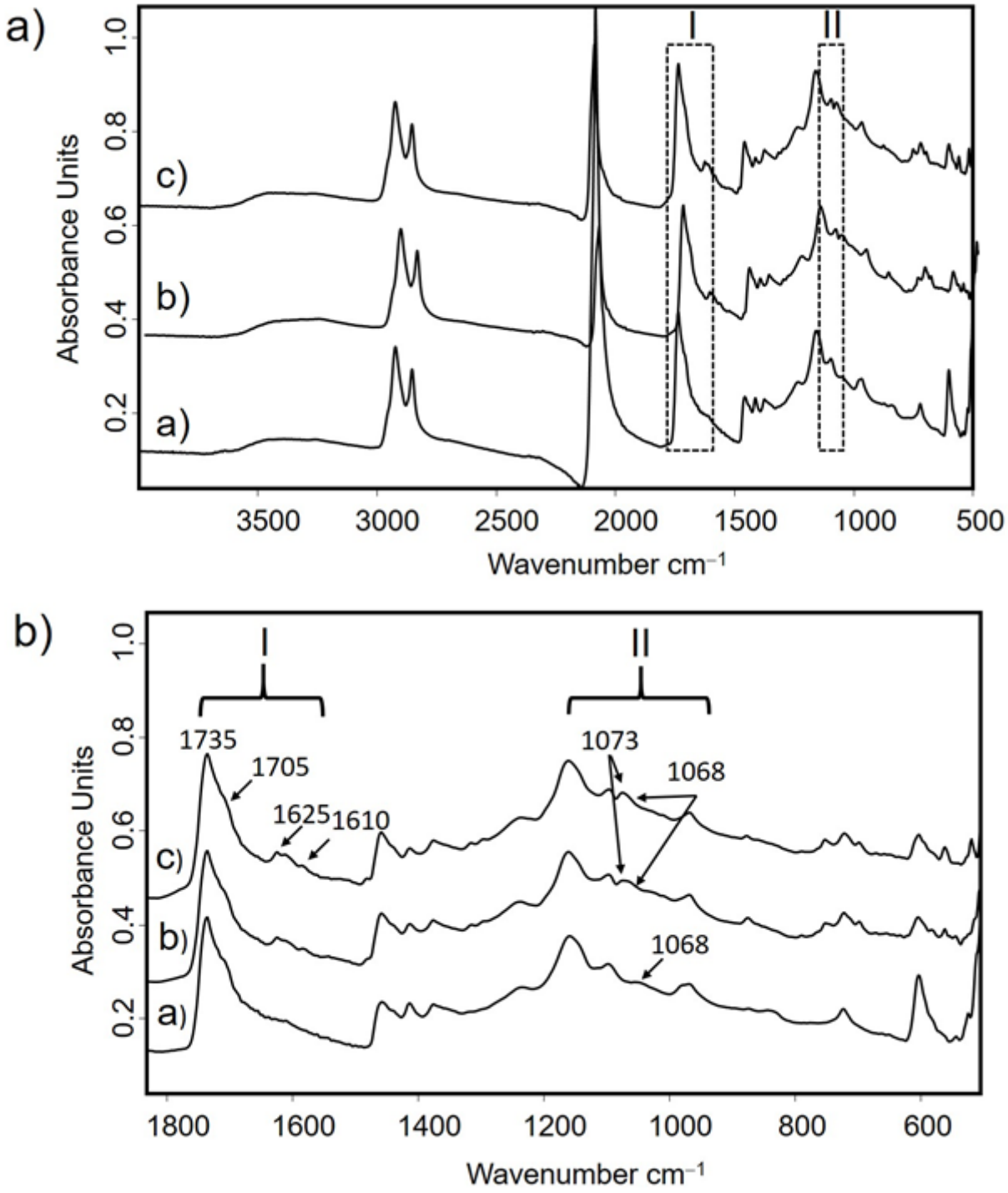

Figure 6

IR absorption spectra of reconstructed paint film specimens indigo+Prussian blue+oil (IPO) a) Entire IR spectrum (4000-600 cm⁻1) b) Detail of the 1800-600 cm⁻1 region For each figure: a) IR spectrum of naturally aged paint film; b) IR spectrum of paint film after UV solar light aging; c) IR spectrum of paint film after UV aging.

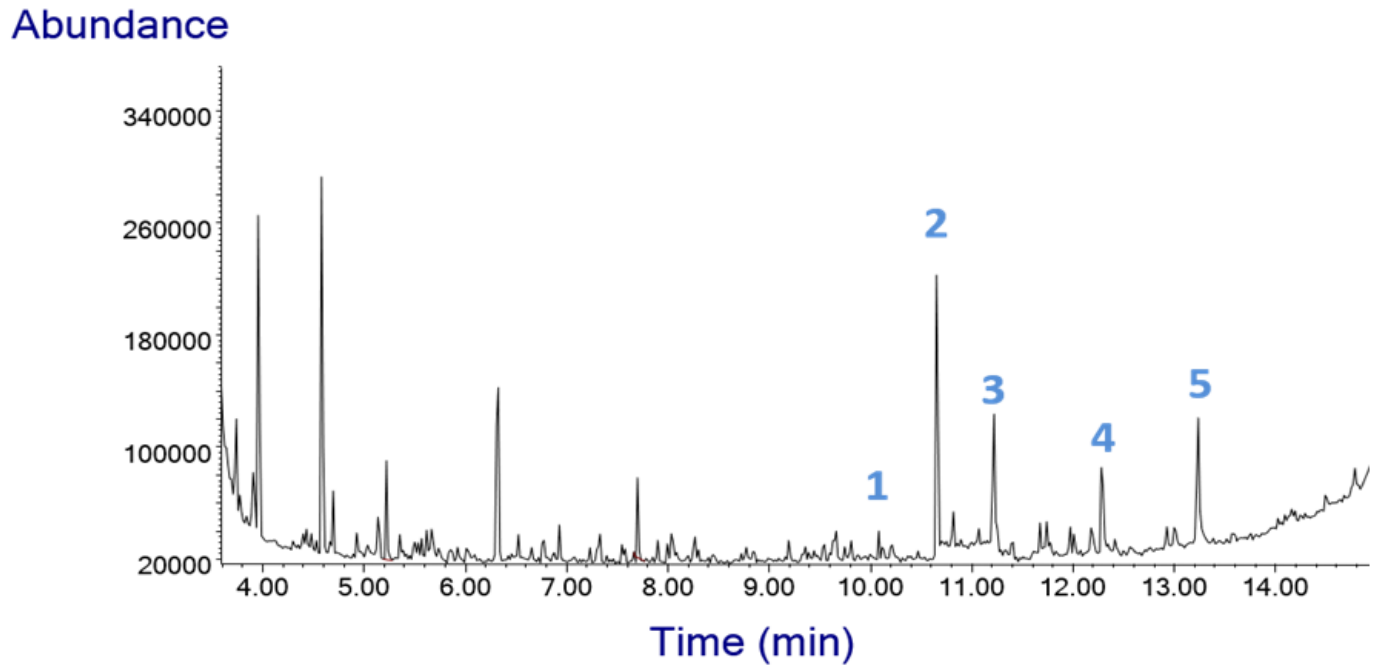

Figure 7

Chromatogram of the altered paint sample. Peaks: octanedioic acid diethyl ester (1), nonanedioic acid diethyl ester (2), decanedioic acid diethyl ester (3), palmitic acid ethyl ester (4) and stearic acid ethyl ester (5).

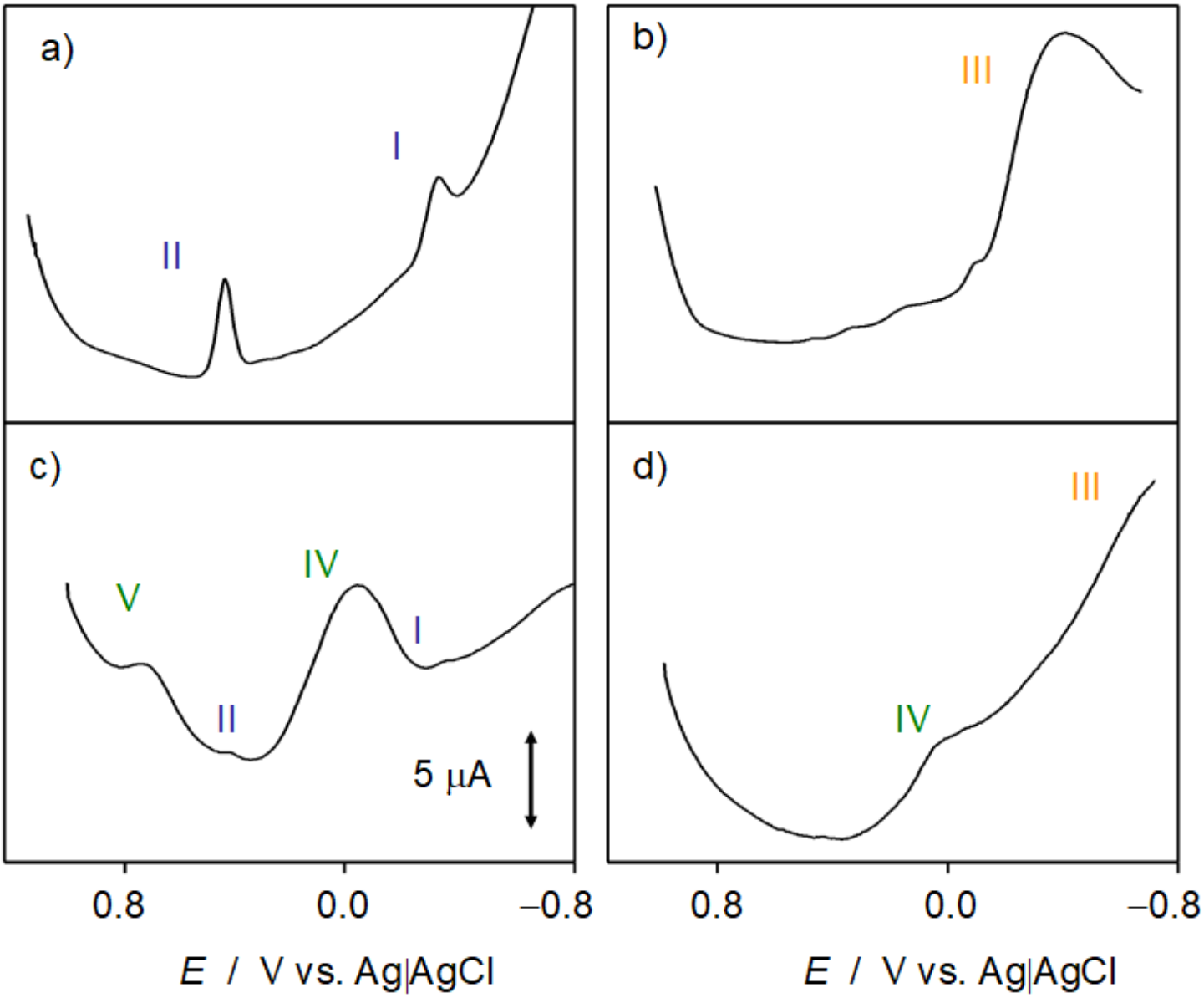

Figure 8

Square wave voltammograms of microparticulate deposits of a) indigo, b) isatin, and submicrosamples extracted from c) unaltered and d) altered layers of the Sant Francesc de Paula paint, all attached to graphite bar immersed into air-saturated 0.25 M HAc/NaAc aqueous buffer at pH 4.75. Potential scan initiated at 1.05 V in the negative direction, potential step increment 4 mV, square wave amplitude 25 mV, frequency 5 Hz.

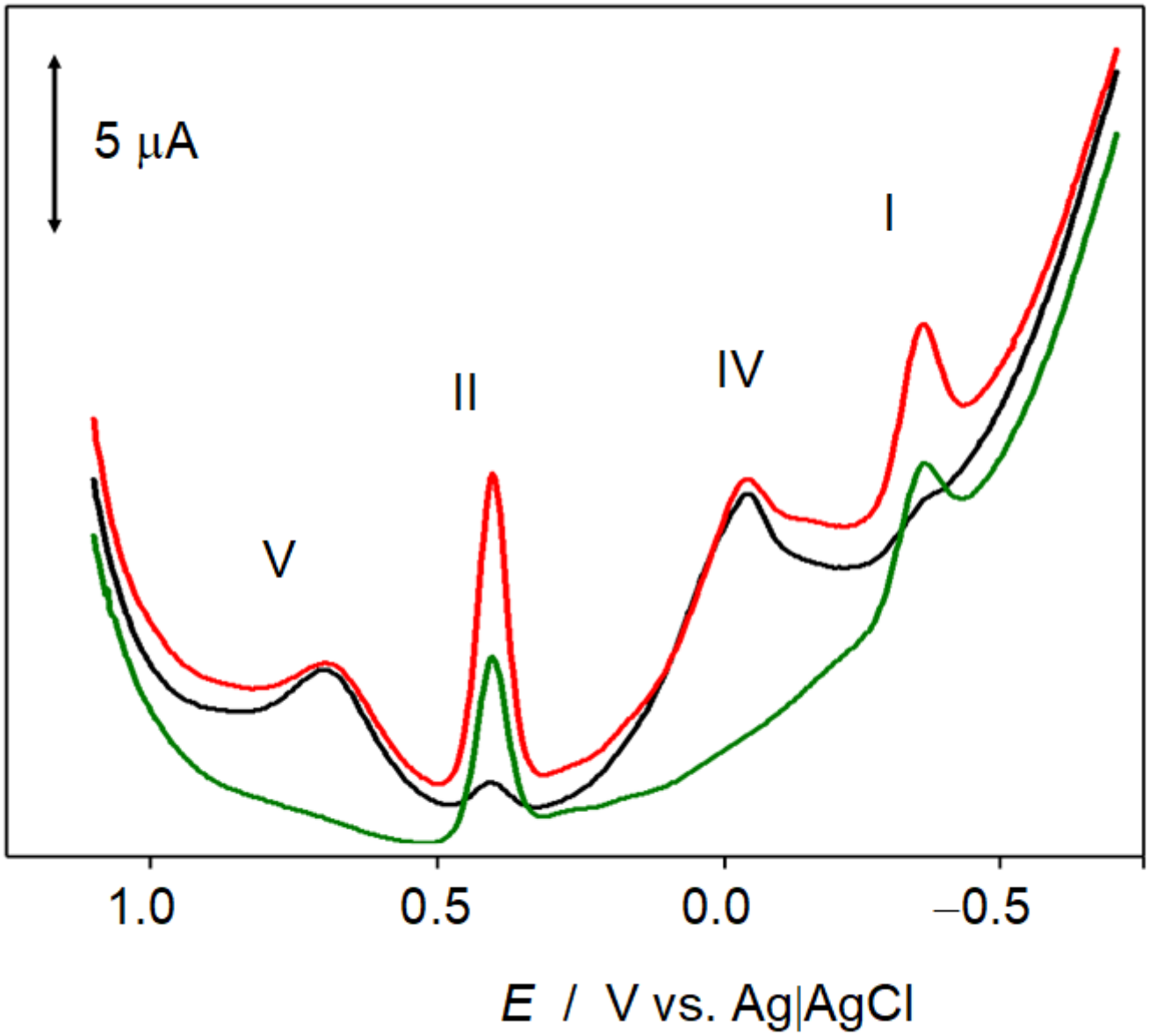

Figure 9

Square wave voltammograms of microparticulate deposits of indigo (green), Prussian blue (black), and a 50% wt mixture of indigo and Prussian blue (red), attached to graphite bar immersed into air-saturated 0.25 M HAc/NaAc solution at pH 4.75. Potential scan initiated at 1.05 V in the negative direction, potential step increment 4 mV, square wave amplitude 25 mV, frequency 5 Hz.

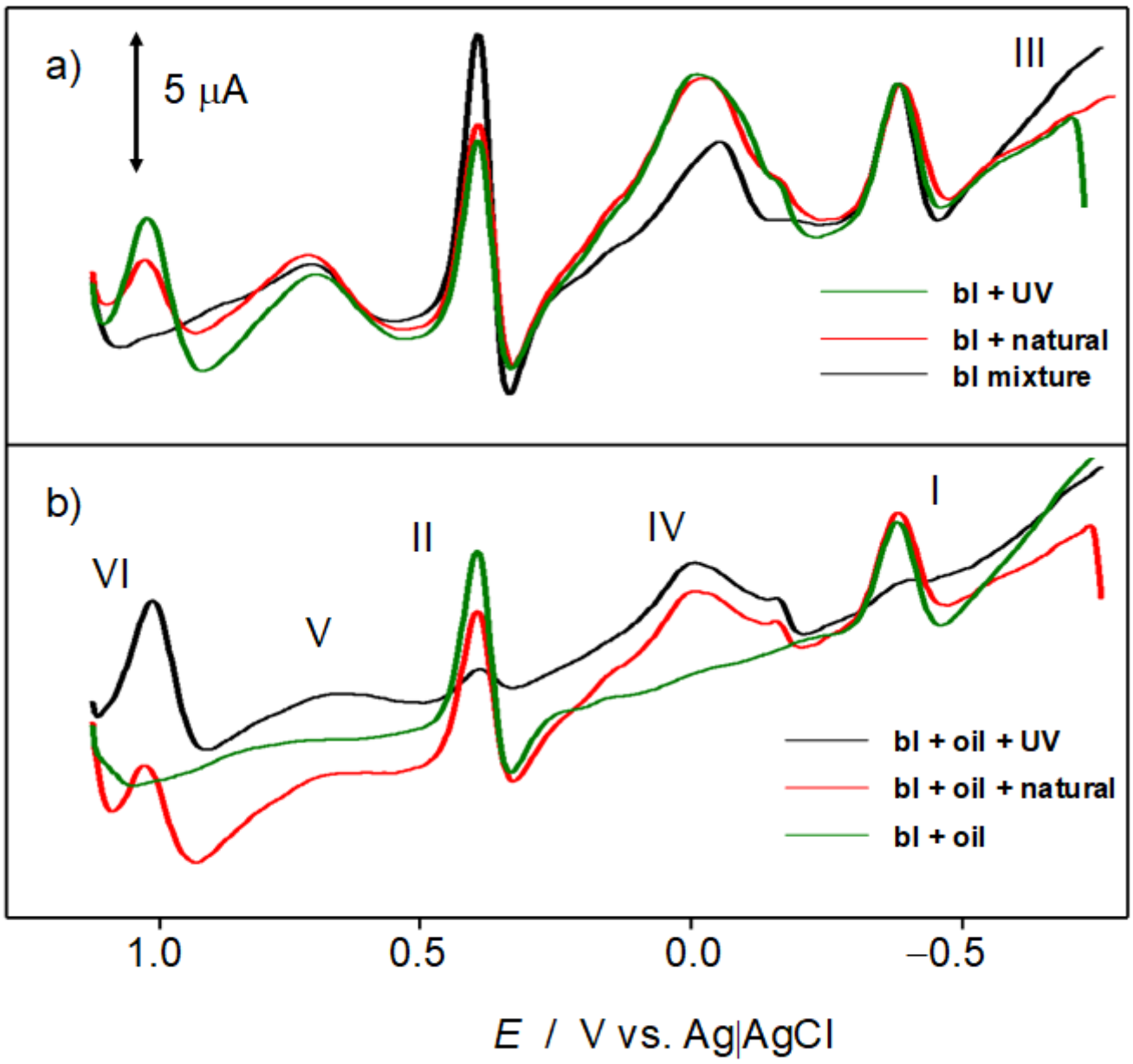

Figure 10

Square wave voltammograms, after semi-derivative convolution, of sample-modified graphite electrodes in contact with air-saturated 0.25 M HAc/NaAc aqueous buffer at pH 4.75. a) 50 %wt indigo plus Prussian blue mixture (labeled as bl) before and after natural and UV solar light aging; b) indigo plus Prussian blue paint film specimens before and after natural and UV solar light aging. Voltammograms in conditions such as in Fig. 9.

Figure 11 was not provided with this version.

Figure 11

Square wave voltammograms of microparticulate deposits of a) indigo, b) isatin, c) indigo paint film specimen after natural aging, d) indigo plus Prussin blue paint specimen after natural aging. Electrolyte: air-saturated 0.25 M HAc/NaAc solution at pH 4.75. Potential scan initiated at 1.05 V in the negative direction, potential step increment 4 mV, square wave amplitude 25 mV, frequency 5 Hz.

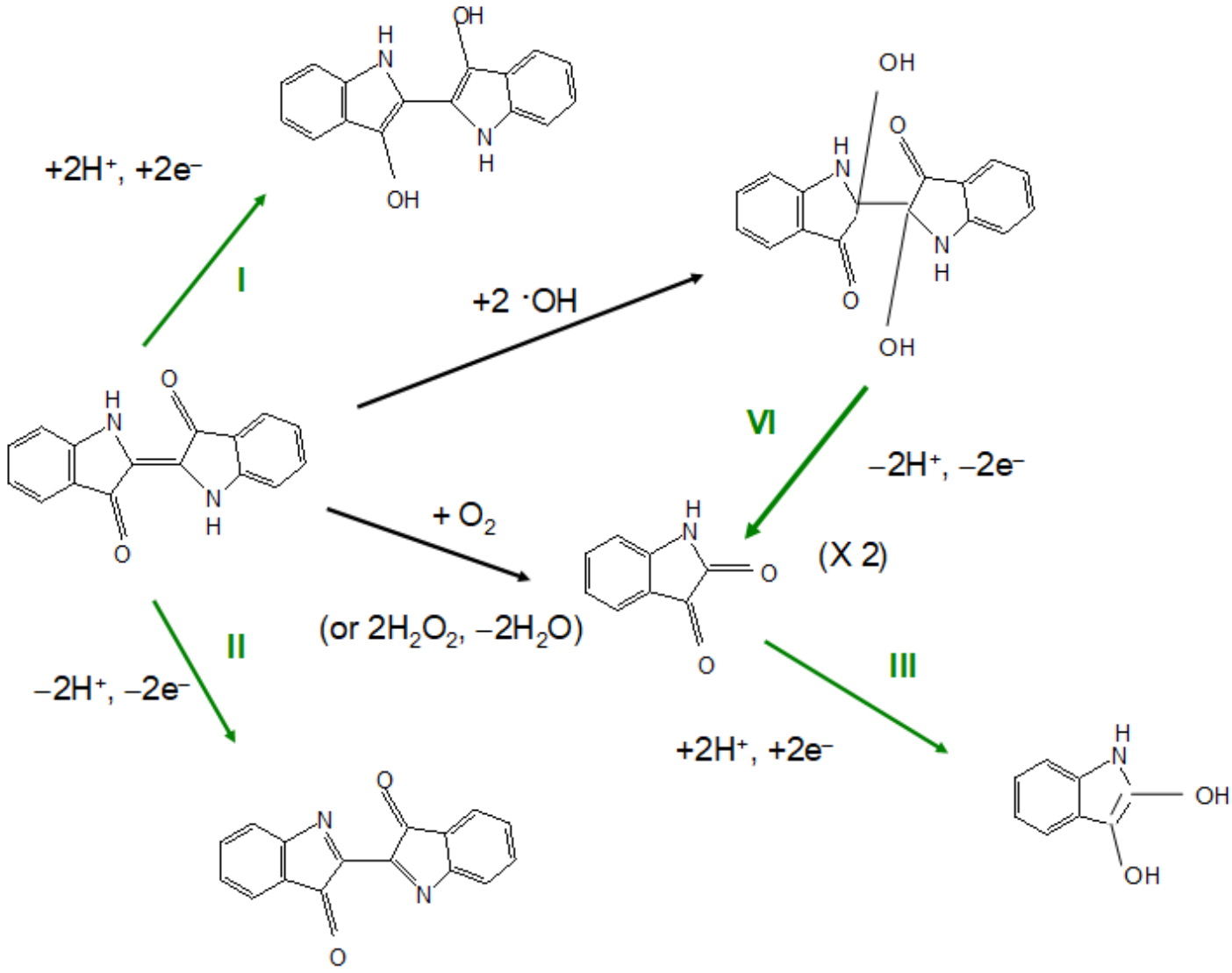

Figure 12

Scheme 1: Molecular representation of the electrochemical (green arrows) and chemical (black arrows) processes involving indigo-related compounds balanced in this study.

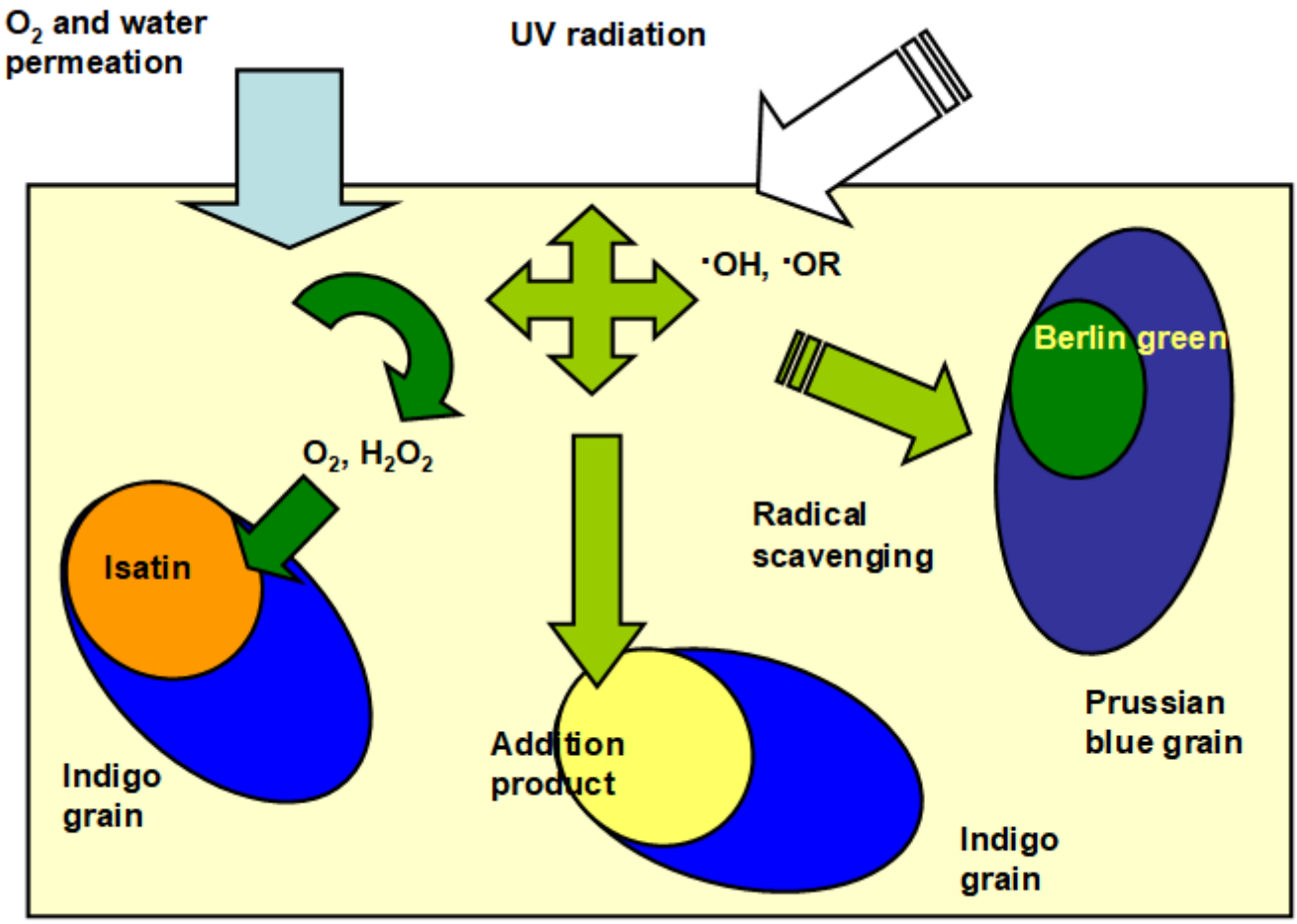

Figure 13

Scheme 2: Schematic representation of the degradation processes in indigo plus Prussian blue oil paints.